Journal of Computational Chemistry

WILEY

Journal of COMPUTATIONAL CHEMISTRY

RESEARCH ARTICLE OPEN ACCESS

AI-Assisted Protein–Peptide Complex Prediction in a Practical Setting

Darren Y. Wang[1] | Luxuan Wang[2] | Andrew Mi[3] | Junmei Wang[2]

[1]High School Student at Hampton Senior High School, Pittsburgh, Pennsylvania, USA | [2]Department of Pharmaceutical Sciences and Computational Chemical Genomics Screening Center, School of Pharmacy, University of Pittsburgh, Pittsburgh, Pennsylvania, USA | [3]High School Student at the School for the Talented and Gifted (TAG), Dallas, Texas, USA

Correspondence: Junmei Wang (junmei.wang@pitt.edu)

Received: 6 May 2025 | **Revised:** 6 May 2025 | **Accepted:** 9 May 2025

Funding: This work was supported by National Institute of General Medical Sciences (R01GM149705) and National Science Foundation (1955260).

Keywords: AlphaFold 2 | ANI-2x | docking protocol | prediction protein–peptide complex in a practical setting | protein–peptide docking | ZDOCK

ABSTRACT

Accurate prediction of protein–peptide complex structures plays a critical role in structure-based drug design, including antibody design. Most peptide-docking benchmark studies were conducted using crystal structures of protein–peptide complexes; as such, the performance of the current peptide docking tools in the practical setting is unknown. Here, the practical setting implies there are no crystal or other experimental structures for the complex, nor for the receptor and peptide. In this work, we have developed a practical docking protocol that incorporated two famous machine learning models, AlphaFold 2 for structural prediction and ANI-2x for ab initio potential prediction, to achieve a high success rate in modeling protein–peptide complex structures. The docking protocol consists of three major stages. In the first stage, the 3D structure of the receptor is predicted by AlphaFold 2 using the monomer mode, and that of the peptide is predicted by AlphaFold 2 using the multimer mode. We found that it is essential to include the receptor information to generate a high-quality 3D structure of the peptide. In the second stage, rigid protein–peptide docking is performed using ZDOCK software. In the last stage, the top 10 docking poses are relaxed and refined by ANI-2x in conjunction with our in-house geometry optimization algorithm—conjugate gradient with backtracking line search (CG-BS). CG-BS was developed by us to more efficiently perform geometry optimization, which takes the potential and force directly from ANI-2x machine learning models. The docking protocol achieved a very encouraging performance for a set of 62 very challenging protein–peptide systems which had an overall success rate of 34% if only the top 1 docking poses were considered. This success rate increased to 45% if the top 3 docking poses were considered. It is emphasized that this encouraging protein–peptide docking performance was achieved without using any crystal or experimental structures.

1 | Introduction

Peptides are becoming an indispensable therapeutic agent class in the small-molecule–dominated world in recent years [1, 2]. According to a survey, there are 22 peptides among the 278 new chemical entities approved by Food and Drug Administration (FDA) from 2016 to 2021 [3]. Peptide drugs are usually more target-specific and potent than small molecule drugs, but they usually have poor ADME (absorption, distribution, metabolism, excretion) profiles [4–6], whereas approved drugs usually have good ADME profiles and fewer adverse effects. Identified oligopeptide inhibitors can also

serve as structural templates for developing small molecule drugs [7, 8]. Thus, it is becoming increasingly important to accurately predict protein–peptide complex structure to facilitate structure-based drug design.

Many protein–peptide docking programs have been developed to study protein–peptide interactions. Critically and comprehensive evaluations of their docking performance have been conducted [9, 10]. Weng et al. evaluated the docking performance for 14 docking programs on 185 protein–peptide complexes. Note that they used ligand-free crystal structures of receptors to evaluate the peptide–protein docking performance, which is a less practical docking setting according to our definition (both the receptor and the ligand structures are unknown). According to their study, the best success rate for top 1 poses is less than 12% for all the studied programs [9]. Agrawal et al. found that FRODOCK [11] and ZDOCK [12] achieve the best ligand-RMSD in blind docking and re-docking, respectively [13]. In recent years, new docking programs or docking strategies have emerged and been tested for more challenging protein–peptide systems. In 2022, Xu and Zou [14] developed a docking protocol coined MDockPeP2 to address the challenge of peptide flexibility in protein–peptide docking studies. Their docking protocol achieved a significantly high success rate of about 70% for the bound-docking on two protein–peptide datasets, peptiDB and LEADS-PEP. However, the success rate dropped dramatically for the unbound docking, 35.9% for peptiDB when top 10 poses were considered. In 2020, Santos et al. developed the DockThor program and tested its performance on the LEADS-PEP dataset. They found that DockThor achieved a success rate of 40% with the overall backbone RMSD below 2.5 Å for the top 1 docking poses; this performance is comparable with that of Glide docking [15]. However, the above docking studies utilized crystal structures of either complexes in terms of re-docking/bound docking or receptors in terms of unbound docking. Their performance is unknown for a more practical setting for which there are no crystal or measured structures for complex, receptor, and peptide.

In 2021, AlphaFold [16], a machine learning (ML)-based protein modeling model has been developed and outperformed many protein modeling tools in critical assessment of protein structure predictions [17]. Recently, a large-scale assessment of AlphaFold 2 (AF2) was conducted for 11 proteomes [18], a major finding is that the ML model can identify rare structural features in Protein Data Bank (PDB) [19] and 25% more residues can be confidently modeled than traditional homology modeling. AlphaFold has been applied to predict peptide structures with amino acid residues between 2 and 50 residues [20]. However, its good performance is achievable only if the peptide sequences have well-defined secondary structures and lack random coils. Tsaban et al. also applied AF2 to model protein–peptide interactions for 96 complexes [21]. They found that AF2 outperformed the state-of-the-art peptide docking protocol PIPER-FlexPepDock; however, their data set might be less challenging as about half of the peptides are helices or strands. It is still unclear whether the performance of AF2 decreases or not when the structures or structure motifs of the receptors and peptides are unseen or uncommon in PDB.

Recently, ML has been applied to develop energy potential mimicking an ab initio chemistry model. A famous example is ANI-2x ML potential mimicking wB97X/6-31G(d) [22, 23]. Although ANI-2x achieves a speedup of ~10^6 factor in comparison to the DFT method, the potential energy surface generated by this ML potential is rough, which causes failures in geometry optimization using the conventional algorithms. Thus, we have developed a conjugate gradient backtracking line search (CG-BS) method which utilizes a more adaptive algorithm to determine the searching steps and directions while ensuring the Wolfe conditions are satisfied, to conquer the difficulty of reaching convergence utilizing ANI-2x [24]. ANI-2x/CG-BS has been applied by us to study the active conformations among the conformational ensembles for PDB ligands [25].

In this work, we proposed a computational protocol to predict protein–peptide complex structures utilizing two famous ML models, AF2 for receptor and ligand structure prediction, and ANI-2x for refining and reranking docking poses. Considering ZDOCK's excellent performance in bound docking, it was applied to generate docking poses prior to ANI-2x/CG-BS refinement. Unlike most protein–peptide docking studies, our protocol does not rely on any crystal structures of the complex, receptor, or peptide. As shown in Figure 1, this docking protocol consists of three major stages. Starting from PDB sequences of receptor and complex (receptor + peptide), AF2 structural prediction is conducted solely for the receptor using monomer mode for a monomeric receptor and multimer mode for a multimeric receptor. AF2 structural prediction is performed for the complex with the multimer mode, and the peptide structure in the 3D-complex structure is extracted. In the second stage, ZDOCK is conducted for the AF2-predicted receptor and peptide structures. In the third stage, the top 10 ZDOCK poses are refined and reranked. We first perform restrained geometric optimization using the AMBER software package, followed by ANI-2x/CG-BS optimization. Last, we re-rank the docking poses according to their ANI-2x potential energies. We evaluated the docking performance using two levels, top 1 and top 3. In the top 1 level, only the best-ranked docking pose according to ANI-2x potential energy is considered, whereas in the top 3 level, the docking pose that best reproduces the peptide conformation in the crystal structure, that is, the smallest Docking RMSD among the top 3 docking poses, is selected for docking performance evaluation. We did not calculate the mean values of RMSDs as this performance metric is much more meaningful when one considers a larger number of docking poses. This docking protocol is assessed by LEADS-PEP [14], which contains 62 challenging protein–peptide systems.

2 | Methodology

2.1 | Datasets Preparation

We compiled a protein–peptide dataset to test our docking performance, which includes all the entries in the LEADS-PEP dataset [14] and nine more to enhance the diversity of the sequence length. The information on the PDB entry and chain ID for the peptide, as well as the amino acid sequence

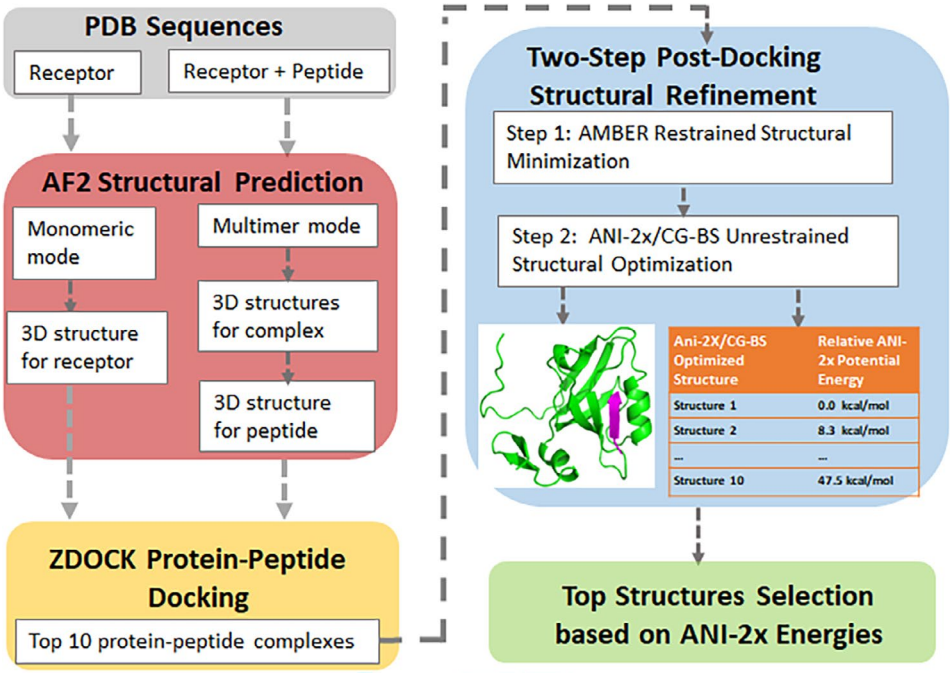

FIGURE 1 | Flowchart of AI-assisted protein–peptide docking in practical setting assuming no crystal structures are available. The protocol consists of three major steps: 3D-structure prediction with AlphaFold 2 (dark red), rigid peptide–protein docking with ZDOCK (yellow), and post-docking structural refinement with AMBER and ANI-2x/CG-BS (blue).

are provided in Table S1. The FASTA files for both receptor and receptor + peptide were prepared for the AF2 structural prediction.

2.2 | AF2 Structural Prediction

We utilized AF2 docker (https://github.com/google-deepmind/alphafold) to conduct structural predictions in two modes, monomer (the default) and multimer. Only the top 1 structure was selected for structural analysis.

2.3 | Protein–Peptide Docking Using ZDOCK

We performed rigid protein–peptide docking using ZDOCK 3.0.2. Each docking run resulted in 2000 docking poses. Only the top 10 docking poses were subjected to post-docking refinement to make the docking protocol efficient.

2.4 | Glide Docking

We followed a standard protocol to conduct a Glide docking study using the standard precision (SP) scoring function. Specifically, Protein Preparation Wizard was first applied to prepare receptor structures by adding missing atoms and adjusting charged residues based on the experimental pH and partial geometry optimization only applying to hydrogen atoms; next, the docking grid was generated with the coordinate center of the co-crystal peptide being the center of the box, and box dimensions are comparable to that of the enclosed peptide; next, flexible docking was conducted with up to 10 docking poses being recorded. In SP docking, we manually rewarded intramolecular hydrogen bonds and enhanced the planarity of conjugated pi groups while keeping the default settings for all other parameters.

2.5 | AMBER-Restrained Structural Minimization

The Leap module of the AMBER 23 [26] software package was applied to generate topologies for the protein–peptide complexes that were described by the FF14SB [27]. The heavy atoms were restrained using a force constant of 1000 kcal/mol/Å^2 during a maximum of 2000 steps of conjugated gradient minimization using the Sander program.

2.6 | ANI-2x/CG-BS Structural Optimization

The AMBER optimized geometries were used to prepare the input file for the subsequent ANI-2x/CG-BS optimization. An ANI-2x/CG-BS optimization was converged when the following criteria were met: The maximum force and RMS force are no greater than 0.00045 and 0.0003 a.u., and the maximum and RMS displacements are no greater than 0.0018 and 0.0012 a.u., respectively. The maximum number of iterations (MAXITER) was set to 10,000. In most cases, ANI-2x/CG-BS optimization converged before the MAXITER condition was met. However, if an optimization was terminated because MAXITER was reached, we restarted the ANI-2x/CG-BS optimization using the restart file.

2.7 | Root-Mean-Square Deviation (RMSD)

As we used the complete amino acid sequences, that is all the gaps in the PDB structures were filled in, to generate more

complete 3D structures using AF2, thus, directly aligning AF2-generated structure to a crystal one via least-square (LS) fitting may be problematic due to the mismatch of the amino acids. We developed an intern program, SPA, an abbreviation for smart protein alignment, to perform protein structural alignment for protein structures with different sequences. SPA takes a sequence alignment of the input and reference proteins so that only the protein positions without gaps can participate in LS fitting. The docking RMSD was calculated as follows: LS-fitting was first performed for the receptor structures; then the resulting transformation matrix was applied to the input peptide structure; last, the RMSD between the transformed input peptide structure and the reference peptide structure was calculated without fitting. Note that all heavy atoms of the peptide participate in the docking RMSD calculations.

A successful structure prediction or a protein–peptide docking prediction is recognized when the RMSD value is smaller than 4 Å for all peptide sequences. This threshold is consistent with the definition of near-native prediction defined by Weng et al., but slightly more stringent for peptides with sequence lengths longer than 10. By using the same criterion of success prediction, we are able to compare the docking performance of our protocol with 14 docking programs recently studied by Weng et al. [9].

3 | Results and Discussion

3.1 | Assessment of AF2 in Modeling the Protein Structures for a Highly Challenging Dataset

The protein–peptide dataset compiled by us included all the 53 entries in the LEADS-PEP dataset, and 9 more were added to increase the coverage of sequence lengths. The 62 entries have amino acid sequence length ranges from 3 to 39. The sequence information of all the entries is shown in Table S1. Most of the peptide structures form random coils; thus, they are highly flexible and mostly adopt random coil secondary structure. There are three major outcomes of the AF2 modeling, either for the single domain receptor (Figure 2) or the multidomain receptor (Figure 3). In Outcome 1, the structure of the complex, receptor, and peptide are very well modeled (yellow for receptor and green for peptide) in comparison with the crystal structure (white for the receptor and red for peptide). In Outcome 2, good RMSD was

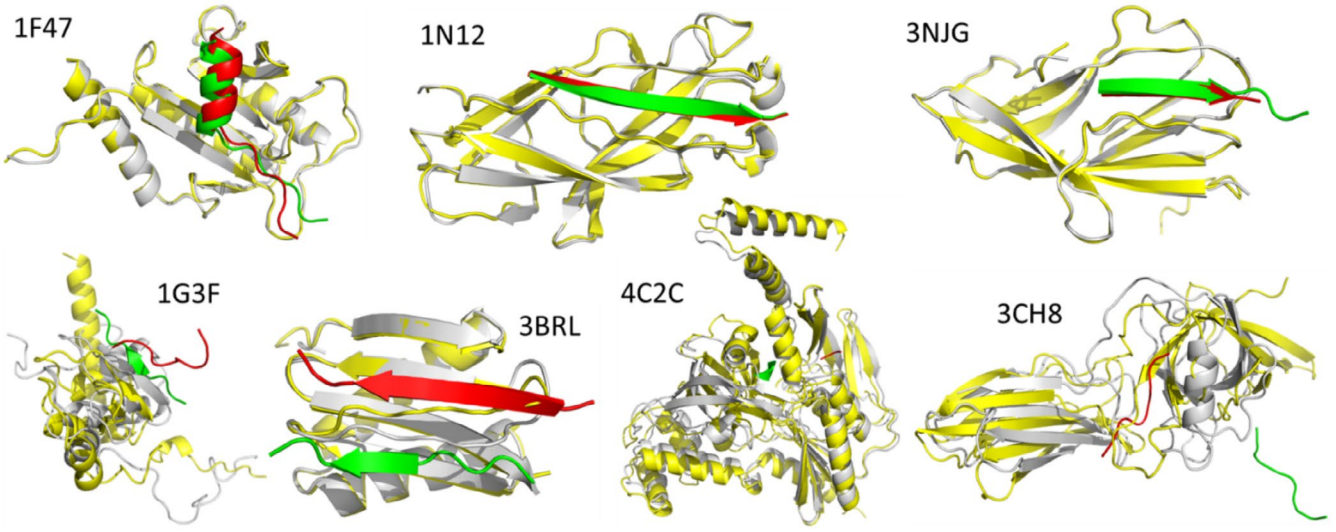

FIGURE 2 | Representative outcomes of AlphaFold 2 modeling for peptides complexed with single domain receptors. Outcome 1: Good RMSDs for receptor, peptide, and complex, represented by 1F47, 1N12, and 3NJG; Outcome 2: Good RMSD for the peptide, bad RMSDs for receptor and complex, represented by 1G3F, 3BRL, and 4C2C; Outcome 3: Good RMSDs for both receptor and peptide, but bad RMSD for the complex, represented by 3CH8.

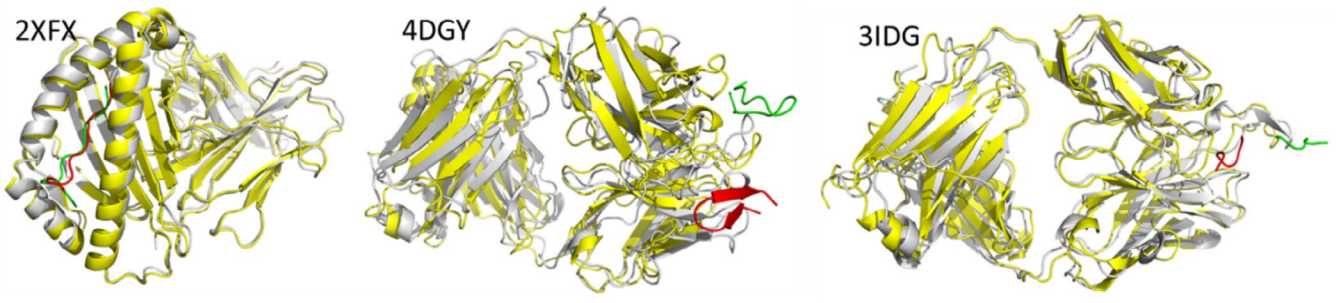

FIGURE 3 | Representative outcomes of AlphaFold modeling for peptides complexed with multi-domain receptors. Outcome 1: Good RMSDs for receptor, peptide, and complex, represented by 2XFX; Outcome 2: Good RMSD for the peptide, bad RMSDs for receptor and complex, represented by 4DGY; Outcome 3: Good RMSDs for both receptor and peptide, but bad RMSD for the complex, represented by 3IDG.

observed only for the peptide, but not for the receptor and complex. In Outcome 3, even though good structures were predicted for the receptor and peptide, the binding mode is incorrect, resulting in a bad complex structure and large Docking RMSD.

The average RMSDs are 2.95, 2.60, and 1.17 Å for the complexes, receptors, and peptides, respectively, and the corresponding success rates are 85%, 87%, and 98% (Table S2). However, the success rate for docking decreased to 74% owing to the scenario of Outcome 3. We also performed AF2 modeling for the receptor and peptide separately (Table S3). Interestingly, the average RMSDs become 2.17 Å for the receptors and 2.20 Å for the peptides. The corresponding success rate increased to 89% for the receptors and decreased to 95% for the ligands. The distributions of the RMSDs are illustrated in Figure 4. It is observed that separately modeling receptors leads to better structures which have smaller RMSDs to the corresponding X-ray structures. On the contrary, the peptide structures from the complex modeling have smaller RMSDs to the corresponding X-ray structures. Representative protein–peptide systems that showcase the above observations are illustrated in Figure 5. Apparently, for the receptor of a system, the blue cartoons from the separate modeling can be better aligned with the white cartoons (the X-ray structures) than the yellow cartoons from the joint modeling of the receptor and peptide. On the other hand, for the peptide of a system, the green cartoons from the joint modeling can be better aligned with the red cartoons (the X-ray structures) than the magenta ones of the separate modeling.

The following is our rationale for the above observation: The AF2 monomer model can result in more accurate structural prediction than the multimer model; thus, separately modeling a

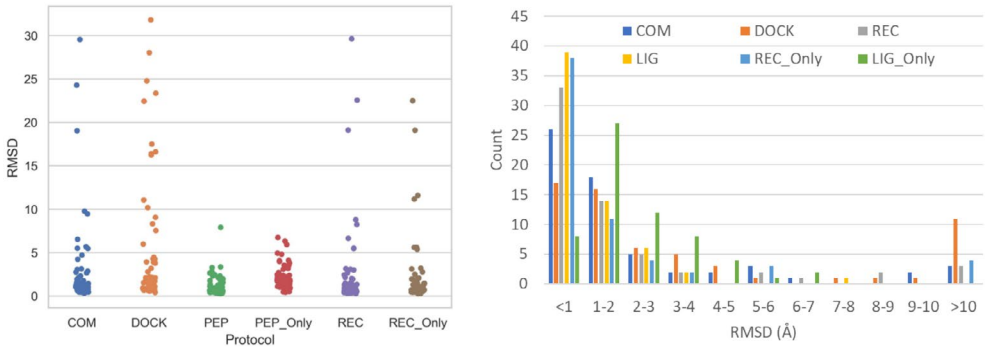

FIGURE 4 | Distributions of RMSDs of complex (COM), receptor (REC, REC_only), peptide (PEP, PEP_only), and docking (DOCK) for RMSD for the best structure predicted by AlphaFold 2. REC_only or PEP_only indicate that the structures were separately modeled for the receptor or peptide using the monomer mode. The scatter distributions of all RMSD values and the column distribution of RMSD ranges are shown in the right and left panels, respectively.

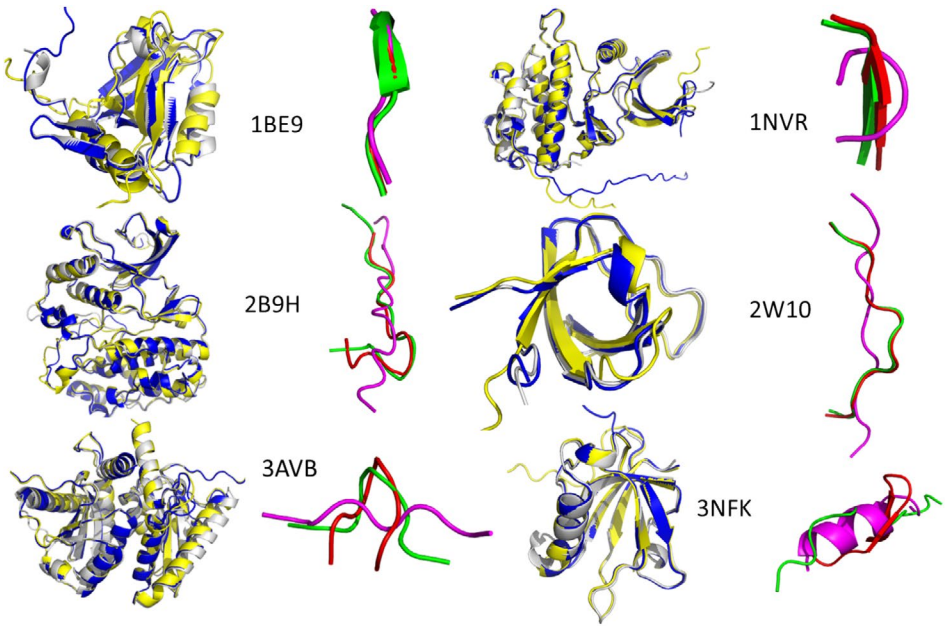

FIGURE 5 | Comparison of two AlphaFold modes (monomer and multimer) in modeling protein–peptide complexes. For each system, the left and right panels show how well the AF2 structures are aligned to the crystal structures for the receptor and the peptide, respectively. Color code for receptors: White for the crystal structures, whereas yellow and blue for the AF2 structures generated with the multimer and monomer modes, respectively. Color code for peptides: Red for the crystal structures, whereas green and magenta for the AF2 structures generated with the multimer and monomer modes, respectively.

receptor leads to more accurate receptor structural prediction, whereas for a peptide, its short sequences may have many template structures in PDB and they may adopt different conformations; thus, modeling the peptide structure in the context of the receptor can result in the receptor-specific conformation for the peptide.

The success rate of protein–peptide docking with AF2, 71%, is very encouraging and comparable to the findings by Tsaban et al. [21] However, this performance may be challenged as those protein–peptide structures were already deposited in the PDB. Thus, we continue to study if we can accurately predict the protein–peptide complexes using docking. In the following Glide or ZDOCK docking studies using AF2 structures, all the receptor structures came from individual modeling, whereas all the peptide structures came from joint modeling of the receptor/peptide complexes with the multimer mode.

3.2 | Prediction of Protein–Peptide Complexes With Glide and ZDOCK

We chose two representative docking programs to conduct protein–peptide docking. Both are mainstream docking programs and achieved good performance in other benchmark studies. As shown in Table S6, the success rate is 33% for the bound docking using the X-ray structures for top 1 level, whereas it increased to 35% for top 3 level. When the AF2 structures were used, as expected, the success rates dropped to 12.5% for top 1 level and top 3 level as well. The distributions of the RMSD ranges for the Glide docking were illustrated in Figure S2. Thus, the Glide docking performance was significantly decreased when modeled structures were applied.

ZDOCK achieved a much better docking performance in a bound docking study with X-ray structures. The success rates are 66% and 73% for top 1 level and top 3 level, respectively. If all the 2000 docking poses were considered, the success rate increased to 94%, indicating ZDOCK can produce correct docking poses for most protein–peptide systems, albeit they are not necessarily top ranked. As expected, the docking performance decreased when AF2 structures were used: The success rates are 27%, 44%, and 76% for top 1 level, top 3 level, and the minimum docking RMSDs in docking pose ensembles, respectively. It is apparent that ZDOCK achieved a much a higher success rate than Glide docking under the same scenario. The distributions of the docking RMSDs are illustrated in Figure 6. The docking RMSDs using both X-ray and AF2 structures were listed in Tables S8 and S9.

3.3 | Post-Docking Refinement and Reranking

Considering the correct docking poses are hidden in the docking pose ensembles produced by ZDOCK, we expect further refinement on those poses with more promising potential function can make those correct docking poses ranked higher. To make this docking protocol efficient, only the top 10 docking poses from ZDOCK were selected to enter the post-docking refinement stage. As shown in Figure 1, the refinement stage consists of two steps: the restrained structural minimization with the AMBER software package [26]. This step can efficiently remove possible clashes in the ZDOCK-generated docking poses while keeping the overall complex structure unchanged. Note that this step can significantly reduce the minimization steps in the subsequent ANI-2x/CG-BS optimization. In the second step, ANI-2x/CG-BS optimization was performed utilizing the default convergence criteria in Gaussian 16 [28]. As shown in Table S9, the two-step refinement and reranking significantly boosted the success rates. For the top 1 level, the mean RMSD decreased from 15.71 to 13.43 Å, whereas the success rate increased from 27% to 34%; for the top 3 level, the mean RMSD decreased from 10.50 to 8.95 Å, whereas the success rate increased from 44% to 45%. Figure 7 illustrated some representative peptide systems with enhanced (Panels A and B) or worsened performance (Panel C).

According to the report by Weng et al. [9], the best top 1 and 10 success rates are 4.3% and 24.3% for global docking, achieved by HPEPDOCK for the peptiDB dataset. Thus, the docking performance of our AI-assisted docking protocol is very encouraging, considering that the high success rates were achieved under a practical setting without using any crystal structures.

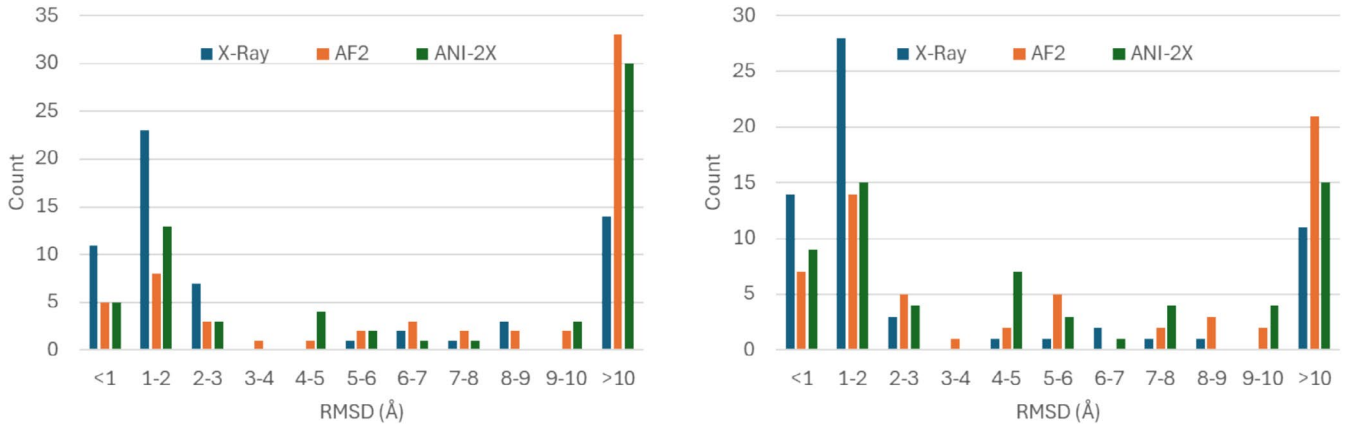

FIGURE 6 | Distributions of best docking RMSDs for ZDOCK using crystal structures (X-Ray) and AlphaFold 2-generated receptor and peptide structures without (AF2) and with post-docking refinement (ANI-2x). Left panel: Only the best docking poses were considered; right panel: The best docking poses in the top 3 docking poses were considered.

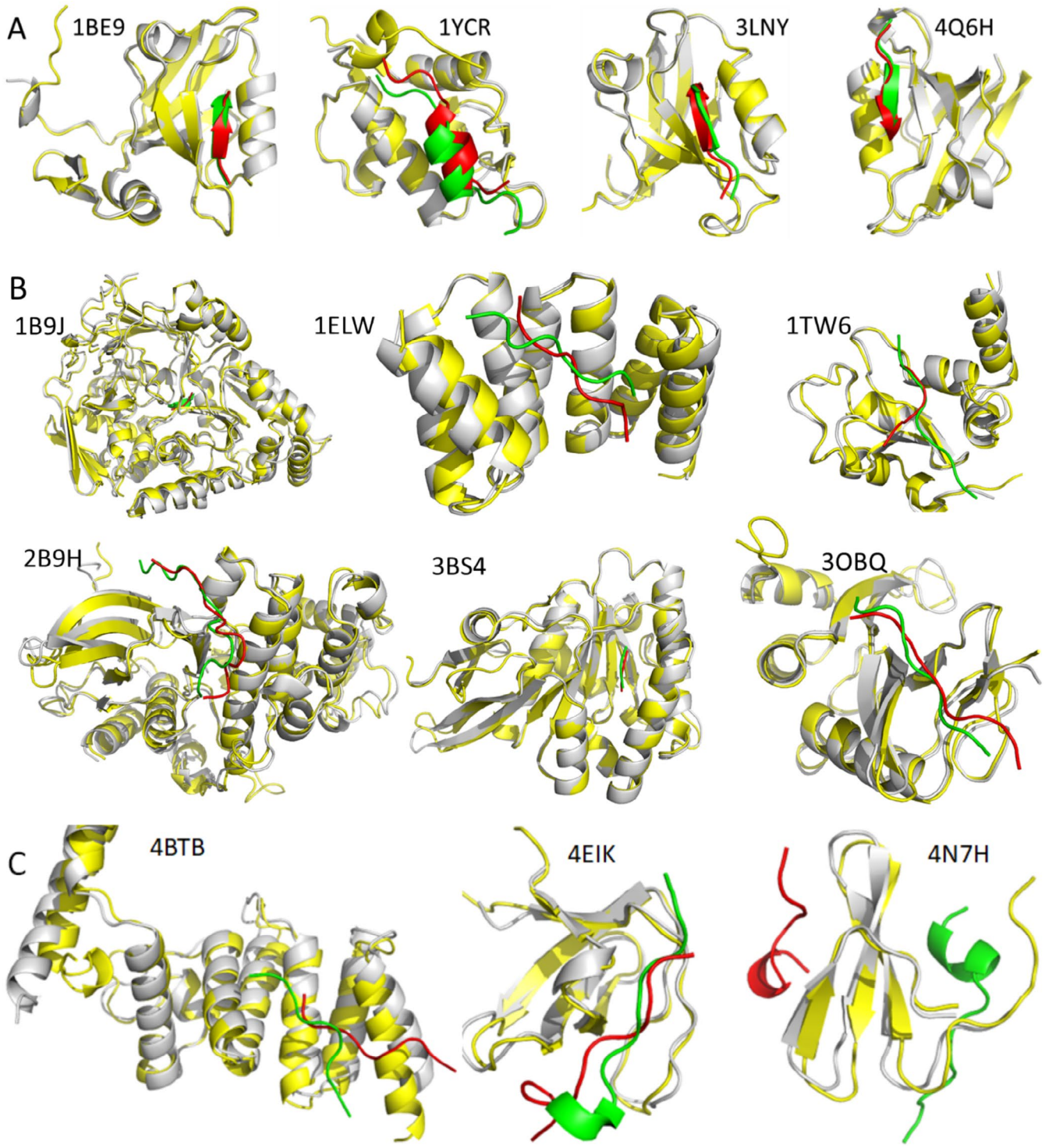

FIGURE 7 | Two scenarios of the AI-assisted docking protocol, either improving the docking performance (A and B) or decreasing the docking performance (C). The peptides adopt secondary structures for the four protein–peptide complexes in (A), which are 1BE9 (0.87 Å), 1YCR (2.74), 3LNY (1.13), and 4Q6H (0.98), respectively. The peptides adopt random coil structures for the six protein–peptide complexes in (B), which are 1B9J (1.47), 1ELW (4.62), 1TW6 (4.74), 2B9H (2.73), 3BS4 (1.70), and 3OBQ (4.30). The protein–peptide systems in (C) have decreased docking performance after ANI-2x structural refinement and reranking, which are 4BTB (9.85), 4EIK (6.62), and 4N7H (21.86). The best RMSDs resulting from the docking protocol are provided for each system. Note that, for the worst scenario for which the docking performance was decreased, good conformations with RMSDs being smaller than 4 Å were among the top 3 conformations for 2B9H (2.77) and 3BS4 (1.26).

The current ANI-2x was developed to reproduce gas phase energies and forces calculated at the wB97X/6-31G(d) level. There is a lack of the description of the solvent effect as well as the entropic effect when a peptide is bound to its receptor in the current ANI-2x potential. It is expected that the successors of ANI-2x, which explicitly consider the solvent effect in the

training process, together with conformational entropy prediction, for example, using WSAS [29], could significantly enhance the success rate of our docking protocol.

In this proof-of-concept study, the docking protocol was assessed by a set of 62 very challenging protein–peptide systems. A systematic evaluation of this protocol and the refined versions (such as using AlphaFold 3 instead of AlphaFold 2) using a larger database, such as peptiDB, and for more docking programs is ongoing and will be reported in the future.

3.4 | Cross-Protein Complex Modeling

It is interesting to investigate the ability of the proposed protocol in identifying non-binders of a given receptor. If the two peptides, one binder and the other a non-binder, share high sequence identity (> 50% for accurate protein modeling), the above protocol should be able to generate similar binding poses for relative binding affinity prediction using free energy-based methods like MM-PBSA [30, 31]. However, if the sequence identity is low, the above protocol may fail. We conducted cross protein–peptide modeling for three pairs of receptors: 1B9J/2B6N, 1BE9/1NVR, and 1G3F/2W0Z. To conduct cross protein–peptide modeling for a pair of receptors P1-L1/P2-L2, we generate P1-L2 and P2-L1 structures using AF2, where L1 is the native peptide of the P1 receptor and L2 is the native peptide of the P2 receptor. L1 and L2 have distinct but the same length of amino acid sequences. As shown in Figure S3, 50% of the mismatched peptides bind to the same sites (1B9J, 1BE9 and 2W0Z), whereas the rest have distant binding modes. The modeling scores, the sum of the predicted template modeling (pTM) and interface predicted template modeling (ipTM), were calculated for the native and mismatched peptides binding to a receptor. The scores of the original peptides are better than the mismatched ones for all receptors except for 1NVR, for which the score is 0.8641 for the mismatched peptide and 0.6379 for the native peptide. As illustrated in Figure S3, the mismatched peptide forms six hydrogen bonds with the receptor, whereas the native peptide only forms four. It is interesting to further validate if the mismatched peptide can truly bind to the receptor. In brief, AF2 can be applied to roughly discriminate binders from non-binders; for those binding to the same site, the relative binding affinities can be further determined by performing binding free energy calculations.

4 | Conclusions

In our study, we developed and evaluated a docking protocol integrated with two famous ML models for predicting protein–peptide complexes in a practical setting using 62 protein–peptide systems. AF2 itself has achieved a very accurate prediction of the protein–peptide complexes, with an overall success rate of 74%. We found that individual modeling of receptor structures can better reproduce the crystal structure of the complex, whereas the joint modeling of receptor and peptide using the multimer mode can facilitate AF2 to generate the receptor-specific peptide structure which can better reproduce the counterpart in the crystal structure of the complex. Our docking protocol using AF2-predicted structures to conduct rigid docking followed by ANI-2x/CG-BS refinement has achieved success rates of 34% for the best docking poses and 45% if the top 3 docking poses were considered. This is a very encouraging docking performance given the fact that it was achieved without using any crystal structures.

Author Contributions

D.Y.W. conducted the research and wrote the manuscript under the guidance of J.W. J.W. conceived the ideas and revised the manuscript. All other co-authors participated in the discussion and revised the manuscript. All authors read and approved the final manuscript.

Acknowledgments

The authors are grateful for the financial support provided by the National Institutes of Health (R01GM149705) to J.W. and the National Science Foundation (1955260) to J.W. The authors would like to thank the computing resources provided by the Center for Research Computing (facility RRID: SCR_022735) at the University of Pittsburgh (NSF award number: OAC-2117681).

Conflicts of Interest

The authors declare no conflicts of interest.

Data Availability Statement

All the experimental protein–peptide structures come from the Protein Data Bank. The protein models were generated by AlphaFold 2 and ZDOCK software. The ANI-2X/CG-BS code for protein reranking can be downloaded freely from https://github.com/junmwang/pyani_mmff.

References

1. L. Wang, N. Wang, W. Zhang, et al., "Therapeutic Peptides: Current Applications and Future Directions," *Signal Transduction and Targeted Therapy* 7, no. 1 (2022): 48.

2. L. Otvos, Jr. and J. D. Wade, "Big Peptide Drugs in a Small Molecule World," *Frontiers in Chemistry* 11 (2023): 1302169.

3. D. Al Shaer, O. Al Musaimi, F. Albericio, and B. G. de la Torre, "2021 FDA TIDES (Peptides and Oligonucleotides) Harvest," *Pharmaceuticals (Basel)* 15, no. 2 (2022): 222.

4. M. Muttenthaler, G. F. King, D. J. Adams, and P. F. Alewood, "Trends in Peptide Drug Discovery," *Nature Reviews. Drug Discovery* 20, no. 4 (2021): 309–325.

5. D. J. Craik, D. P. Fairlie, S. Liras, and D. Price, "The Future of Peptide-Based Drugs," *Chemical Biology & Drug Design* 81, no. 1 (2013): 136–147.

6. A. C. Lee, J. L. Harris, K. K. Khanna, and J. H. Hong, "A Comprehensive Review on Current Advances in Peptide Drug Development and Design," *International Journal of Molecular Sciences* 20, no. 10 (2019): 2383.

7. M. D. King, T. Long, D. L. Pfalmer, T. L. Andersen, and O. M. McDougal, "SPIDR: Small-Molecule Peptide-Influenced Drug Repurposing," *BMC Bioinformatics* 19, no. 1 (2018): 138.

8. P. L. Scognamiglio, C. Di Natale, G. Perretta, and D. Marasco, "From Peptides to Small Molecules: An Intriguing but Intricated Way to New Drugs," *Current Medicinal Chemistry* 20, no. 31 (2013): 3803–3817.

9. G. Q. Weng, J. B. Gao, Z. Wang, et al., "Comprehensive Evaluation of Fourteen Docking Programs on Protein-Peptide Complexes," *Journal of Chemical Theory and Computation* 16, no. 6 (2020): 3959–3969.

10. F. Berenger, A. Voet, X. Y. Lee, and K. Y. J. Zhang, "A Rotation-Translation Invariant Molecular Descriptor of Partial Charges and Its

Use in Ligand-Based Virtual Screening," *Journal of Cheminformatics* 6, no. 1 (2014): 1–2.

11. E. Ramirez-Aportela, J. R. Lopez-Blanco, and P. Chacon, "FRODOCK 2.0: Fast Protein-Protein Docking Server," *Bioinformatics* 32, no. 15 (2016): 2386–2388.

12. B. G. Pierce, K. Wiehe, H. Hwang, B. H. Kim, T. Vreven, and Z. Weng, "ZDOCK Server: Interactive Docking Prediction of Protein-Protein Complexes and Symmetric Multimers," *Bioinformatics* 30, no. 12 (2014): 1771–1773.

13. P. Agrawal, H. Singh, H. K. Srivastava, S. Singh, G. Kishore, and G. P. S. Raghava, "Benchmarking of Different Molecular Docking Methods for Protein-Peptide Docking," *BMC Bioinformatics* 19, no. Suppl 13 (2019): 426.

14. X. Xu and X. Zou, "Predicting Protein-Peptide Complex Structures by Accounting for Peptide Flexibility and the Physicochemical Environment," *Journal of Chemical Information and Modeling* 62, no. 1 (2022): 27–39.

15. T. A. Halgren, R. B. Murphy, R. A. Friesner, et al., "Glide: A New Approach for Rapid, Accurate Docking and Scoring. 2. Enrichment Factors in Database Screening," *Journal of Medicinal Chemistry* 47, no. 7 (2004): 1750–1759.

16. J. Jumper, R. Evans, A. Pritzel, et al., "Highly Accurate Protein Structure Prediction With AlphaFold," *Nature* 596, no. 7873 (2021): 583–589.

17. L. M. F. Bertoline, A. N. Lima, J. E. Krieger, and S. K. Teixeira, "Before and After AlphaFold2: An Overview of Protein Structure Prediction," *Frontiers in Bioinformatics* 3 (2023): 3.

18. M. Akdel, D. E. Pires, E. P. Pardo, et al., "A Structural Biology Community Assessment of AlphaFold2 Applications," *Nature Structural & Molecular Biology* 29, no. 11 (2022): 1056.

19. H. M. Berman, J. Westbrook, Z. Feng, et al., "The Protein Data Bank," *Nucleic Acids Research* 28, no. 1 (2000): 235–242.

20. E. F. McDonald, T. Jones, L. Plate, J. Meiler, and A. Gulsevin, "Benchmarking AlphaFold2 on Peptide Structure Prediction," *Structure* 31, no. 1 (2023): 111–119.e2.

21. T. Tsaban, J. K. Varga, O. Avraham, Z. Ben-Aharon, A. Khramushin, and O. Schueler-Furman, "Harnessing Protein Folding Neural Networks for Peptide-Protein Docking," *Nature Communications* 13, no. 1 (2022): 176.

22. J. S. Smith, O. Isayev, and A. E. Roitberg, "ANI-1: An Extensible Neural Network Potential With DFT Accuracy at Force Field Computational Cost," *Chemical Science* 8, no. 4 (2017): 3192–3203.

23. C. Devereux, J. S. Smith, K. K. Huddleston, et al., "Extending the Applicability of the ANI Deep Learning Molecular Potential to Sulfur and Halogens," *Journal of Chemical Theory and Computation* 16, no. 7 (2020): 4192–4202.

24. D. Hao, X. He, A. E. Roitberg, S. Zhang, and J. Wang, "Development and Evaluation of Geometry Optimization Algorithms in Conjunction With ANI Potentials," *Journal of Chemical Theory and Computation* 18, no. 2 (2022): 978–991.

25. F. Han, D. Hao, X. He, L. Wang, T. Niu, and J. Wang, "Distribution of Bound Conformations in Conformational Ensembles for X-Ray Ligands Predicted by the ANI-2X Machine Learning Potential," *Journal of Chemical Information and Modeling* 63, no. 21 (2023): 6608–6618.

26. D. A. Case, H. M. Aktulga, K. Belfon, et al., "How to Cite Amber," (2023), San Francisco: University of California.

27. J. A. Maier, C. Martinez, K. Kasavajhala, L. Wickstrom, K. E. Hauser, and C. Simmerling, "ff14SB: Improving the Accuracy of Protein Side Chain and Backbone Parameters From ff99SB," *Journal of Chemical Theory and Computation* 11, no. 8 (2015): 3696–3713.

28. M. J. T. Frisch, H. B. Schlegel, G. E. Scuseria, et al., *Gaussian 16, Revision B.01* (Gaussian Inc, 2016).

29. J. Wang and T. Hou, "Develop and Test a Solvent Accessible Surface Area-Based Model in Conformational Entropy Calculations," *Journal of Chemical Information and Modeling* 52, no. 5 (2012): 1199–1212.

30. Y. Sun, X. He, T. Hou, L. Cai, V. H. Man, and J. Wang, "Development and Test of Highly Accurate Endpoint Free Energy Methods. 1: Evaluation of ABCG2 Charge Model on Solvation Free Energy Prediction and Optimization of Atom Radii Suitable for More Accurate Solvation Free Energy Prediction by the PBSA Method," *Journal of Computational Chemistry* 44, no. 14 (2023): 1334–1346.

31. E. Wang, H. Sun, J. Wang, et al., "End-Point Binding Free Energy Calculation With MM/PBSA and MM/GBSA: Strategies and Applications in Drug Design," *Chemical Reviews* 119, no. 16 (2019): 9478–9508.

Supporting Information

Additional supporting information can be found online in the Supporting Information section.